EFFECT OF INDISTINGUISHABLE NUCLEI ON PRODUCT ROTATIONAL DISTRIBUTIONS: D+DI→D_2+I

Klaus-Dieter RINNEN, Dahv A.V. KLINER, Mark A. BUNTINE and Richard N. ZARE
Department of Chemistry, Stanford University, Stanford, CA 94305, USA

Received 16 February 1990; in final form 16 April 1990

A marked population alternation between adjacent rotational levels is observed for the $D_2(v=1, J)$ product of the D+DI→D_2+I reaction, analogous to that reported for the H+HI→H_2+I reaction (P.M. Aker, G.J. Germann, and J.J. Valentini, J. Chem. Phys. 90 (1989) 4795; D.A.V. Kliner, K.-D. Rinnen and R.N. Zare, J. Chem. Phys. 90 (1989) 4625). These alternations result from the indistinguishability of the D (H) nuclei in the D+DI (H+HI) reaction. The magnitude of the alternations indicates that there are no symmetry constraints on the reaction complex aside from nuclear exchange symmetry (conserved nuclear spin-statistics (CNSS) condition).

1. Introduction

Theoretical treatments of bimolecular chemical reactions often treat the nuclei as being distinguishable. However, in reactions that involve two or more identical particles, this treatment must be modified. This modification is required to satisfy the generalized Pauli exclusion principle [1], namely, the total wavefunction, Ψ_{tot}, for the system is unchanged for the exchange of two identical bosons and changes sign for the exchange of two identical fermions. The resulting constraints and their effect on chemical reactions are well known theoretically [2–5]. These effects were experimentally demonstrated as early as 1928 in the rotational energy-transfer fluorescence spectrum resulting from collisions of He atoms with electronically excited I_2 molecules [6]. However, direct experimental confirmation in reactive collisions has been sparse. Most prior studies have been concerned with the effect of nuclear indistinguishability in photofragmentation processes (half collisions) [7–16] or have presented indirect evidence of this effect [17]. The first direct observation of the influence of nuclear indistinguishability on a bimolecular chemical reaction was made for the H+HI→H_2+I reaction [18,19], in which a marked population alternation was found between adjacent rotational levels of the nascent H_2 product.

We report here measurements of the isotopically related reaction system, D+DI→D_2+I. The $D_2(v=1, J)$ product quantum state distribution again exhibits pronounced population alternations between adjacent rotational levels. While even J levels are more populated for the D_2 product, odd J levels are more populated for the H_2 product. The conditions necessary to produce these oscillations are discussed.

2. Experimental

The experimental apparatus has been described previously [20–22]. Purified DI (see below) flows into a vacuum chamber through a quartz nozzle (4 Torr backing pressure). The molecular beam is crossed by two counterpropagating laser beams approximately 1 mm below the tip of the nozzle. The first laser (Spectra Physics, DCR-1A, Nd:YAG, 266 nm, 10 Hz) photolyzes a portion of the DI gas. Under typical photolysis conditions of ≈3.0 mJ pulse energy in a 2.5 mm beam, approximately 10% of the DI molecules are photodissociated. This process generates fast D atoms with center-of-mass collision energies of 1.59 and 0.67 eV in the population density ratio of 0.74:0.26 [23,24]. The two D-atom energies correspond to competing photodissociation

0009-2614/90/$ 03.50

channels leading to the production of $I(^2P_{3/2})$ and $I^*(^2P_{1/2})$, respectively. As the classical barrier to reaction is only 0.04 eV [25], both D-atom channels can lead to reaction.

The nascent D_2 product distribution is measured via (2+1) resonance-enhanced multiphoton ionization (REMPI). In this process, the D_2 molecules resonantly absorb two photons ($\lambda \approx 210$ nm) to undergo a transition from the $X\,^1\Sigma_g^+$ (v, J) ground state to the E, F $^1\Sigma_g^+$ $(v'_E=0, J'=J)$ excited electronic state. Here $v'_E=0$ denotes the lowest vibrational level in the E well of the E, F state. Subsequent absorption of an additional photon of the same wavelength leads to ionization of the electronically excited D_2. The ions are mass selectively detected in a shuttered time-of-flight mass spectrometer [26]. The time-gated ion signal is collected with a computer-interfaced CAMAC-based data acquisition system [27].

The 210 nm radiation necessary for state-selective detection of D_2 is obtained by frequency tripling (INRAD, Autotracker II) a Nd:YAG-pumped dye laser (Spectra Physics, DCR-3G; PDL-1; dye: Excition, R640/DCM) using β-barium borate crystals [#1]. The firing of the probe laser is delayed by approximately 55 ns with respect to the photolysis laser. At this delay, the product distribution has been shown to be unperturbed by subsequent collisions or product fly-out from the reaction volume [20–22].

In the absence of the photolysis laser, D_2^+ ions are still detected [21]. This is caused by photolysis of DI induced by the probe laser, i.e. the probe laser both generates D atoms and detects the D_2 product formed during a single laser pulse. The resulting probe-laser-induced product signal must be subtracted from the observed signal in order to obtain the desired quantum-state distribution for the D+DI reaction at a fixed photolysis wavelength (266 nm). Therefore, a shot-by-shot subtraction scheme is applied, as discussed in detail in ref. [22] (method 2).

To assure that the observed D_2 results exclusively from the D+DI reaction, special attention is given to the purity as well as to the storage of the DI gas prior to and during the experiment. The DI (Cambridge Isotope Laboratories; stated purity: D, 99%) is purified in a glass bulb by a freeze–pump–thaw cycle to remove the D_2 contaminant; most of the I_2 contaminant remains in the DI cylinder. The purified DI is stored in a sample cylinder that is Teflon lined to minimize wall exchange reactions. Exposure of the DI reagent to light is avoided to suppress DI decomposition. In our study of the H+HI reaction using the same apparatus [19,28], it was determined that after ≈ 10 h of storage the partial pressure of H_2 caused by HI decomposition was less than 3% of the HI pressure. A similar decomposition rate is expected for DI. The surfaces of the gas handling system are passivated by exposure to DI for several hours when switching from the H+HI to the D+DI reaction.

3. Results

We recorded the ion signal for the $D_2(v=1, J=0$–$24)$ product from the D+DI reaction. To obtain the quantum-state population distributions from the recorded spectra, it was necessary to determine the relationship between ion signals and relative quantum-state populations under our experimental conditions. Therefore, the detection procedure was calibrated against an effusive, hot nozzle source in a separate experiment. The results of this calibration have been published elsewhere [29,30].

Application of calibration factors to the observed distributions generates the quantum-state distributions listed in tables 1 and 2 and plotted in figs. 1 and 2. There are three types of entries in these tables:

(i) *Populations, i.e. calibrated ion signals.* These are denoted by the entries without parentheses (solid circles in figs. 1 and 2).

(ii) *Estimated populations, i.e. ion signals with estimated calibration factors.* The range of calibrated rotational levels is smaller than that populated by the reaction. For the calibrated levels, the experimental correction factors are in close agreement with those derived from calculated two-photon cross sections [30]. For most of these levels, the experimentally and theoretically determined factors are unity; it is found that there are strong deviations in the two-

[#1] The barium borate crystals were supplied by R.S. Feigelson and R.K. Route and grown as part of a research program sponsored in part by the Army Research Office, contract DAAL03-86-K-0129, and in part by the NSF/MRL Program through the Center for Materials Research, Stanford University.

Table 1
H_2 rotational state populations [a] for $H+HI \rightarrow H_2(v=1)+I$ at center-of-mass collision energies of 3.0 eV and 2.1 eV in the ratio of 0.64:0.36

J	Observed	Nuclear spin corrected
0	(0.0029±0.0003)	(0.013 ±0.001)
1	(0.019 ±0.001)	(0.013 ±0.001)
2	0.012 ±0.001	0.024 ±0.002
3	0.046 ±0.002	0.031 ±0.002
4	0.021 ±0.002	0.042 ±0.003
5	0.080 ±0.004	0.054 ±0.003
6	0.028 ±0.001	0.057 ±0.003
7	0.093 ±0.005	0.062 ±0.003
8	0.039 ±0.001	0.078 ±0.003
9	0.144 ±0.008	0.097 ±0.006
10	0.068 ±0.004	0.138 ±0.008
11	0.216 ±0.011	0.145 ±0.008
12	[0.050 ±0.002]	[0.101 ±0.005]
13	(0.097 ±0.013)	(0.065 ±0.009)
14	[0.013 ±0.002]	[0.026 ±0.004]
15	(0.049 +0.001)	(0.033 +0.001)
16	(0.0075±0.0006)	(0.015 ±0.001)
17	[0.0073±0.0004]	[0.0049±0.0003]
18	(0.0036±0.0004)	(0.0073±0.0008)
19	[0.0013±0.0001]	[0.0009±0.0001]
20	[0.0003±0.0001]	[0.0006±0.0001]
21	[0.0012±0.0001]	[0.0008±0.0001]

[a] Error bars represent one standard deviation. The numbers in parentheses denote those levels for which the calibration factors are taken as unity, in accord with theoretical predictions. The numbers in square brackets denote uncalibrated ion signals; see text.

photon cross sections for levels that have non-unit correction factors. Therefore, for uncalibrated levels where the two-photon cross sections predict unit correction factors, we applied factors of unity. These levels, namely, $J=0$–3, 15–19 for $D_2(v=1)$ and $J=0$–2, 15, 16, 18 for $H_2(v=1)$, are denoted by parentheses in the tables (open circles in figs. 1 and 2).

(iii) *Uncalibrated ion signals.* Estimated correction factors were not determined for uncalibrated levels that are theoretically predicted to have non-unit correction factors. For these levels, the measured ion signals are reported. Experimental calibration factors would be necessary to convert their values to populations. These entries are not included in figs. 1 and 2, but are denoted by square brackets in tables 1 and 2. Note that the level $D_2(v=1, J=20)$ is excluded because it is not resolved spectroscopically from the $D_2(v=2, J=12)$ transition in the (2+1) REMPI detection scheme.

Table 2
D_2 rotational state populations [a] for $D+DI \rightarrow D_2(v=1)+I$ at center-of-mass collision energies of 3.1 eV and 2.1 eV in the ratio of 0.74:0.26

J	Observed	Nuclear spin corrected
0	(0.012±0.002)	(0.009±0.002)
1	(0.003±0.001)	(0.005±0.001)
2	(0.011±0.002)	(0.008±0.002)
3	0.006±0.002	0.010±0.002
4	0.018±0.003	0.013±0.002
5	0.010±0.002	0.015±0.002
6	0.028±0.003	0.021±0.002
7	0.014±0.002	0.021±0.002
8	0.036±0.002	0.026±0.002
9	0.019±0.001	0.028±0.002
10	0.046±0.003	0.034±0.002
11	0.027±0.002	0.040±0.002
12	0.063±0.003	0.047±0.002
13	0.035±0.003	0.051±0.004
14	0.089±0.007	0.066±0.006
15	(0.050±0.003)	(0.074±0.005)
16	(0.119±0.010)	(0.088±0.007)
17	(0.066±0.007)	(0.098±0.010)
18	(0.131±0.012)	(0.096±0.009)
19	(0.051±0.003)	(0.075±0.005)
20	–	–
21	[0.039±0.002]	[0.058±0.003]
22	[0.077±0.007]	[0.056±0.005]
23	[0.024±0.002]	[0.035±0.003]
24	[0.018±0.004]	[0.013±0.003]
25	[0.008±0.001]	[0.012±0.002]

[a] Error bars represent one standard deviation. The numbers in parentheses denote those levels for which the calibration factors are taken as unity, in accord with theoretical predictions. The numbers in square brackets denote uncalibrated ion signals; see text.

4. Discussion

The calibrated product state distributions are shown in fig. 1. The two reactions examined, $H+HI \rightarrow H_2+I$ and $D+DI \rightarrow D_2+I$, are exothermic by 1.42 eV and 1.46 eV, respectively [25,31]. The total energies available to the reaction products for photolysis at 266 nm are 3.0 (2.1 eV) for H+HI and 3.1 (2.1 eV) for D+DI for the high (low) collision energy channel. These energies are sufficient to form highly rotationally excited product molecules in $v=1$.

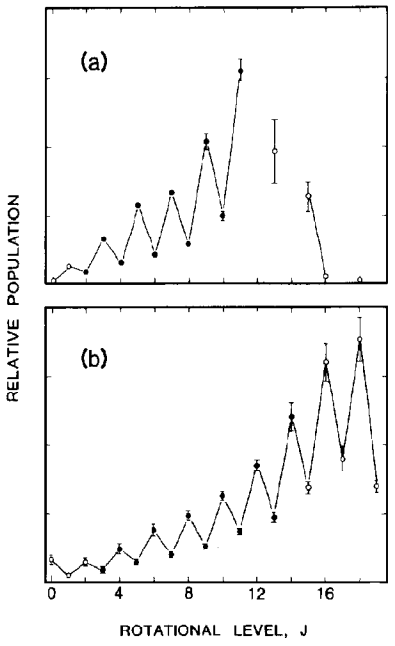

Fig. 1. Product rotational distributions from the chemical reactions: (a) $H+HI \rightarrow H_2(v=1, J)+I$ and (b) $D+DI \rightarrow D_2(v=1, J)+I$. The solid symbols denote populations (i.e. calibrated ion signals). The open symbols indicate the populations of levels for which the calibration factors are taken as unity, in accord with theoretical predictions: see text. Error bars represent one standard deviation.

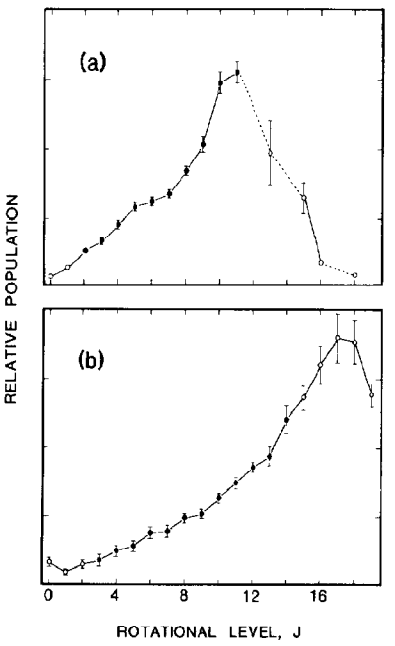

Fig. 2. Product rotational distribution from the chemical reactions: (a) $H+HI \rightarrow H_2(v=1, J)+I$ and (b) $D+DI \rightarrow D_2(v=1, J)+I$. The distributions are corrected for the indistinguishability of the H and D nuclei in the H+HI and D+DI reaction, respectively; see fig. 1. In (a) the populations of odd J levels have been divided by three to account for the ortho:para ratio of 3:1. In (b) the populations of even J levels have been divided by two to account for the ortho:para ratio of 1:2. The open symbols indicate the populations of levels for which the calibration factors are taken as unity, in accord with theoretical predictions; see text. Error bars represent one standard deviation.

High rotational excitation has also been observed by Aker, Germann and Valentini [18]. We defer a discussion of the reaction dynamics of the H+HI reaction family to a future publication [28]. Instead, we concentrate here on the most remarkable feature of this study, namely, the striking alternations in population as a function of product rotational level. In this context, the H+HI and D+DI reactions provide an illustration of the consequences of nuclear indistinguishability in bimolecular chemical reactions.

To understand the experimental observations, it is necessary to examine the symmetry constraints placed on chemical reactions involving identical nuclei. Consider the process

$$A+AB \rightarrow [A_2B] \rightarrow A_2+B\,,$$

where A is an atom, B is an atom or molecule, and $[A_2B]$ denotes the transitory (short- or long-lived) collision complex. Permutation symmetry of the indistinguishable nuclei A in $[A_2B]$ requires the total wavefunction, Ψ_{tot}, to change sign upon interchange of the nuclei A if A is a fermion (nuclear spin $I=1/2, 3/2, \ldots$), such as the H nucleus. In contrast, if A is a boson ($I=0, 1, \ldots$), like the D nucleus, the sign of the wavefunction remains unchanged under nuclear interchange.

Specific consequences of the constraints that arise from the interchange of indistinguishable nuclei become apparent upon factoring Ψ_{tot} into a nuclear spin part, Ψ_{nuc}, and a part that depends upon all other degrees of freedom (rotational, vibrational, and electronic), Ψ_{other}. This factorization is valid for collision complexes that have a small coupling between Ψ_{nuc} and Ψ_{other}. In particular, such reaction systems

exhibit a small hyperfine depolarization constant, and/or proceed via a mechanism in which the lifetime of the reaction complex $[A_2B]$ is short compared to the interaction time between Ψ_{nuc} and Ψ_{other}. Because of the small coupling between Ψ_{nuc} and Ψ_{other}, nuclear spin is a constant of the motion for the reaction; hence, the overall nuclear spin symmetry is unchanged during the collision process. The H+HI reaction family provides a case for which this assumption is valid.

The behavior of the total wavefunction under interchange of the indistinguishable nuclei may now be determined by considering separately the transformation properties of Ψ_{nuc} and Ψ_{other}.

4.1. Symmetry constraints implied by Ψ_{nuc}

The factorization of Ψ_{tot} allows us to consider the reaction as proceeding via potential energy surfaces that are labelled in terms of their nuclear spin permutation symmetry. For the case of a reaction involving two indistinguishable nuclei, there are two distinct nuclear spin symmetries; hence there are two such surfaces. One surface leads to formation of molecules in symmetric nuclear spin states (ortho surface), while the other leads to the formation of antisymmetric nuclear spin states (para surface). These two surfaces are energetically degenerate except for the hyperfine splitting. The more complicated cases of reactions involving three or more identical nuclei are treated in refs. [2–4].

On the basis of nuclear spin conservation, assumed above, reaction trajectories do not hop between these surfaces during the course of a reaction. Therefore, trajectories on each surface are independently subject to the symmetry constraints associated with Ψ_{other}. The weighting factors for the two sets of trajectories are a product of factors derived from symmetry constraints implied by Ψ_{other}, as well as from nuclear spin statistics. The nuclear spin degeneracy of the ortho surface relative to that of the para surface is $(I+1):I$ if A is a fermion (H nucleus) and $I:(I+1)$ if A is a boson (D nucleus). Here, I is the spin quantum number of the nucleus.

The existence of two surfaces is demonstrated for example in the photofragmentation experiments of Schramm, Bamford, and Moore [8]. These workers excited formaldehyde to the $2^1 4^1$ vibrational band of the S_1 state, which leads to photodissociation. The excitation of a particular ortho- (para-)formaldehyde line selects a surface with distinct nuclear spin permutation symmetry. For photodissociation via the $2^1 4^1$ vibrational state, ortho- (para-)H_2CO almost exclusively yields ortho- (para-)H_2 as a photofragment.

4.2. Dynamical preferences implied by Ψ_{other}

It must be examined whether the collision process has a dynamical preference for either of the two reaction surfaces in order to determine any scaling factors associated with constraints implied by Ψ_{other}. If the reaction proceeds via a complex with a preferred collision symmetry (geometry) for nuclear permutation/inversion, then Ψ_{other} imposes additional symmetry constraints on the reaction system [3,4]. Hence, there will be an additional weighting factor in addition to that derived from nuclear spin statistics.

If the reaction complex does not have a preferred collision symmetry with respect to nuclear permutation/inversion, then there are no additional constraints on the reaction system. In this case, which we call the conserved nuclear spin-statistics (CNSS) condition, the reaction products exhibit solely the effects of nuclear spin statistics, i.e. the ratio of the collisions occurring on the ortho surface relative to the collisions occurring on the para surface is the same for reactive collisions as for all collisions, reactive and nonreactive. In particular, the product rotational distributions will reflect the degeneracies of the ortho and para levels.

The CNSS condition is expected to be general and applicable to most chemical collision processes. As mentioned earlier, the validity of the CNSS condition requires: (a) small coupling between Ψ_{other} and Ψ_{nuc}, and (b) no dynamical bias in the collision complex. Requirement (a) is well documented by the observation of conservation of nuclear spin in inelastic collisions [6,32], and photofragmentation [7–16]. Presently, no experimental results contradict requirement (b).

In order to assess the influence of the symmetry constraints implied by Ψ_{nuc} and Ψ_{other} on the $H+HI \rightarrow H_2+I$ and $D+DI \rightarrow D_2+I$ reactions, the ortho and para product quantum-state distributions for

the two reactions are first scaled by the weighting factors derived from nuclear spin statistics. This procedure isolates the effects resulting from Ψ_{other}.

It is found that this scaling smoothes the product quantum-state distributions (fig. 2). For the H+HI reaction, the indistinguishable H nuclei have a nuclear spin of 1/2. Nuclear spin statistics therefore weight the odd J levels three times more than the even J levels. When the distribution is corrected accordingly by dividing the odd J level populations by three, the rotational distribution becomes smooth within experimental uncertainty (fig. 2a). In the case of the D+DI reaction, however, the indistinguishable D nuclei have a nuclear spin of 1. Nuclear spin statistics weight the even J levels by a factor of two with respect to the odd J levels. Scaling of the even J level populations by the appropriate weight factor of two again results in a smooth distribution for the D_2 product (fig. 2b).

Since the population alternations disappear within experimental uncertainties when the nuclear spin symmetry is taken into account, we conclude that the observed structure in the product rotational distributions is purely a consequence of nuclear spin symmetry in the D+DI and the H+HI reactions. It therefore appears that the weighting between the "ortho" and "para" trajectory sets is not affected by any symmetry constraints derived from the reaction complex. The collision complex fulfills the CNSS condition.

Our experimental observations of the H+HI and D+DI reactions provide evidence for the generality of the CNSS condition to chemical reactions. The observation of a dynamical bias in a chemical system would indicate severe restrictions on the collision complex and/or the existence of dynamical resonances. Further studies of reactions involving indistinguishable nuclei are necessary to search for possible violations of the CNSS condition.

Acknowledgement

We are grateful to W.M. Huo for providing us with the results of her calculations of the E–X two-photon transition moments for H_2 and D_2. We thank P.H. Vaccaro and W.J. van der Zande for many helpful discussions and for proof-reading this manuscript. DAVK gratefully acknowledges a National Science Foundation graduate fellowship. This project is supported by the National Science Foundation under Grant No. NSF CHE 87-05131.

Note added

Recently, the role of indistinguishable nuclei has been investigated for the ion–molecule reaction of H^+ with H_2 in the two ortho-to-para ratios of 3:1 and $\approx$1:3 [33]. This study has demonstrated for this reaction system the validity of the CNSS condition, which was referred to as the frozen nuclear spin (FNS) approximation.

References

[1] P.R. Bunker, Molecular symmetry and spectroscopy (Academic Press, New York, 1979).
[2] W.H. Miller, J. Chem. Phys. 50 (1969) 407.
[3] M. Quack, Mol. Phys. 34 (1977) 477.
[4] M. Quack, in: Symmetries and properties of non-rigrid molecules: a comprehensive survey, eds. J. Maruani and J. Serre (Elsevier, Amsterdam, 1983) p. 355.
[5] V.Z. Kresin and W.A. Lester Jr., Chem. Phys. Letters 159 (1989) 297.
[6] R.W. Wood and F.W. Loomis, Phil. Mag. 6 (1928) 231.
[7] M. Péalat, D. Debarre, J.-M. Marie, J.-P.E. Taran, A. Tramier and C.B. Moore, Chem. Phys. Letters 98 (1983) 299.
[8] B. Schramm, D.J. Bamford and C.B. Moore, Chem. Phys. Letters 98 (1983) 305.
[9] D. Debarre, M. Lefebvre, M. Péalat, J.-P.E. Taran, D.J. Bamford and C.B. Moore, J. Chem. Phys. 83 (1985) 4476.
[10] J.J. Valentini, D.P. Gerrity, D.L. Phillips, J.-C. Nieh and K.D. Tabor, J. Chem. Phys. 86 (1987) 6745;
J.J. Valentini, J. Chem. Phys. 86 (1987) 6757.
[11] N. Halberstadt, J.A. Beswick and K.C. Janda, J. Chem. Phys. 87 (1987) 3966.
[12] J.I. Cline, N. Sivakumar, D.D. Evard and K.C. Janda, Phys. Rev. A 36 (1987) 1944.
[13] J.I. Cline, B.P. Reid, D.D. Evard, N. Sivakumar, N. Halberstadt and K.C. Janda, J. Chem. Phys. 89 (1988) 3535.
[14] D.D. Evard, C.R. Bieler, J.I. Cline, N. Sivakumar and K.C. Janda, J. Chem. Phys. 89 (1988) 2829.
[15] J.I. Cline, N. Sivakumar, D.D. Evard, C.R. Bieler, B.P. Reid, N. Halberstadt, S.R. Hair and K.C. Janda, J. Chem. Phys. 90 (1989) 2605.
[16] R. Ogorzalek Loo, H.P. Haerri, G.E. Hall and P.L. Houston, J. Chem. Phys. 90 (1989) 4222.

[17] J.E. Heidenreich and M.H. Thiemens, J. Chem. Phys. 84 (1986) 2129;
S.K. Bains-Sahota and M.H. Thiemens, J. Phys. Chem. 91 (1987) 4370.
[18] P.M. Aker, G.J. Germann and J.J. Valentini, J. Chem. Phys. 90 (1989) 4795.
[19] D.A.V. Kliner, K.-D. Rinnen and R.N. Zare, J. Chem. Phys. 90 (1989) 4625.
[20] R.S. Blake, K.-D. Rinnen, D.A.V. Kliner and R.N. Zare, Chem. Phys. Letters 153 (1988) 365.
[21] K.-D. Rinnen, D.A.V. Kliner, R.S. Blake and R.N. Zare, Chem. Phys. Letters 153 (1988) 371.
[22] K.-D. Rinnen, D.A.V. Kliner and R.N. Zare, J. Chem. Phys. 91 (1989) 7514.
[23] R.D. Clear, S.J. Riley and K.R. Wilson, J. Chem. Phys. 63 (1974) 1340.
[24] I. Levy and M. Shapiro, J. Chem. Phys. 89 (1988) 2900.
[25] M. Baer and I. Last, in: Potential energy surfaces and dynamics calculations, ed. D.G. Truhlar (Plenum Press, New York, 1981).
[26] K.-D. Rinnen, D.A.V. Kliner, R.S. Blake and R.N. Zare, Rev. Sci. Instr. 60 (1989) 717.
[27] R.S. Blake, Ph.D. Thesis, Department of Chemistry, Stanford University, Stanford, CA (1988).
[28] D.A.V. Kliner, K.-D. Rinnen, M.A. Buntine and R.N. Zare, unpublished results.
[29] K.-D. Rinnen, D.A.V. Kliner, R.N. Zare and W.M. Huo, Israel J. Chem. 29 (1989) 369.
[30] W.M. Huo, private communication;
K.-D. Rinnen, D.A.V. Kliner, M.A. Buntine, R.N. Zare and W.M. Huo, unpublished results.
[31] H. Umemoto, S. Nakagawa and S. Tsunashima, Chem. Phys. 124 (1988) 259.
[32] P. Pringsheim, Fluorescence and phosphorescence (Wiley, New York, 1965), and references therein.
[33] D. Gerlich, J. Chem. Phys. 92 (1990) 2377.